



## Clastic sediment flux to tropical Andean lakes: records of glaciation and soil erosion

Donald T. Rodbell<sup>a,\*</sup>, Geoffrey O. Seltzer<sup>b,\*</sup>, Bryan G. Mark<sup>c</sup>, Jacqueline A. Smith<sup>d</sup>, Mark B. Abbott<sup>e</sup>

<sup>a</sup> Geology Department, Union College, Schenectady, NY 12308, USA

<sup>b</sup> Department of Earth Sciences, Syracuse University, Syracuse, NY 13244-1070, USA

<sup>c</sup> Department of Geography, The Ohio State University, Columbus, OH 43210, USA

<sup>d</sup> Department of Physical and Biological Sciences, The College of Saint Rose, Albany, NY 12203, USA

<sup>e</sup> Department of Geology and Planetary Science, University of Pittsburgh, Pittsburgh, PA 15260-3332, USA

### ARTICLE INFO

#### Article history:

Received 30 August 2006

Received in revised form

12 May 2008

Accepted 1 June 2008

### ABSTRACT

We developed records of clastic sediment flux to 13 alpine lakes in Peru, Ecuador, and Bolivia, and compared these with independently dated records of regional glaciation. Our objectives are to determine whether a strong relationship exists between the extent of ice cover in the region and the rate of clastic sediment delivery to alpine lakes, and thus whether clastic sediment records serve as reliable proxies for glaciation during the late Pleistocene. We isolated the clastic component in lake sediment cores by removing the majority of the biogenic and authigenic components from the bulk sediment record, and we dated cores by a combination of radiocarbon and tephrochronology. In order to partially account for intra-basin differences in sediment focusing, bedrock erosivity, and sediment availability, we normalized each record to the weighted mean value of clastic sediment flux for each respective core. This enabled the stacking of all 13 lake records to produce a composite record that is generally representative of the tropical Andes. There is a striking similarity between the composite record of clastic sediment flux and the distribution of ~100 cosmogenic radionuclide (CRN) exposure ages for erratics on moraine crests in the central Peruvian and northern Bolivian Andes. The extent of ice cover thus appears to be the primary variable controlling the delivery of clastic sediment to alpine lakes in the region, which bolsters the increasing use of clastic sediment flux as a proxy for the extent of ice cover in the region. The CRN moraine record and the stacked lake core composite record together indicate that the expansion of ice cover and concomitant increase in clastic sediment flux began at least 40 ka, and the local last glacial maximum (LLGM) culminated between 30 and 20 ka. A decline in clastic sediment flux that began ~20 ka appears to mark the onset of deglaciation from the LLGM, at least one millennium prior to significant warming in high latitude regions. The interval between 20 and 18 ka was marked by near-Holocene levels of clastic sediment flux, and appears to have been an interval of much reduced ice extent. An abrupt increase in clastic sediment flux 18 ka heralded the onset of an interval of expanded ice cover that lasted until ~14 ka. Clastic sediment flux declined thereafter to reach the lowest levels of the entire length of record during the early–middle Holocene. A middle Holocene climatic transition is apparent in nearly all records and likely reflects the onset of Neoglaciation and/or enhanced soil erosion in the tropical Andes.

© 2008 Elsevier Ltd. All rights reserved.

## 1. Introduction

### 1.1. Late Quaternary glaciation of the tropical Andes

The timing of glacier margin fluctuations during the last glacial–deglacial cycle and Holocene in the tropical Andes has

\* Corresponding author. Tel.: +1 518 388 6034; fax: +1 518 388 6417.

E-mail addresses: [rodbelld@union.edu](mailto:rodbelld@union.edu) (D.T. Rodbell), [mark.9@osu.edu](mailto:mark.9@osu.edu) (B.G. Mark), [smithj@strose.edu](mailto:smithj@strose.edu) (J.A. Smith), [abbott1@pitt.edu](mailto:abbott1@pitt.edu) (M.B. Abbott).

\* Deceased.

received considerable attention during the last three decades. Recent global compilations and comparisons of the magnitude of snowline depression during this interval (Smith et al., 2005a; Rodbell et al., 2008) highlight the continued need for improved chronologic control for the glacial landforms that are the basis for reconstructions of past snowlines in this region. Furthermore, since the high-activity-ratio glaciers of the tropical Andes respond rapidly to climatic perturbations, glacial deposits in this region may be especially useful in determining the role of the tropics in the abrupt climatic oscillations that have been documented in polar regions (e.g., Stocker, 2002). However, no single proxy

indicator provides a continuous archive of oscillations in glacier margins; in the following paragraphs we review several of the best-dated records.

Estimates of the age of the local last glacial maximum (LLGM) have been substantially improved by recent cosmogenic radionuclide (CRN;  $^{10}\text{Be}$  and  $^{26}\text{Al}$ ) dating of 182 erratics on moraine crests from piedmont and valley glaciers and two bedrock exposures in the drainage basins of Laguna Junin (Peru) and Lago Titicaca (Peru/Bolivia; Fig. 1; Smith et al., 2005b,c). These studies suggest that glaciers reached their maximum LLGM extent  $\sim 30$  ka and had retreated upvalley from the maximum positions by  $\sim 20$  ka. In addition, two sets of moraines were generated approximately midway through the last deglaciation  $\sim 18$ – $14$  and  $\sim 14$ – $11$  ka. In the Junin drainage basin, moraines that delineate LLGM ice positions are located several kilometers upvalley from much older moraines that yielded numerous (40) CRN ages  $> 200$  ka (Smith et al., 2005b,c). Although Smith et al. (2005b,c) assert that their CRN chronology provides evidence that the LLGM predates the global LGM as defined by SPECMAP (Martinson et al., 1987) or by EPILOG (Mix et al., 2001), the discontinuous nature of the moraine record coupled with age uncertainties of  $\pm 10$ – $15\%$  preclude a detailed comparison of the timing of the onset or termination of the LLGM in the tropical Andes with that in other regions or with the SPECMAP and EPILOG reconstructions.

Seltzer et al. (2000, 2002) used the magnetic susceptibility (MS) of sediment cores from Laguna Junin and Lago Titicaca as a proxy for glacial flour concentration and glacier extent in the valleys that drain into these lakes. Laguna Junin and Lago Titicaca are located in intermontane basins and have not been overrun by ice for at least  $\sim 200$  ka. According to Seltzer et al. (2002), the abrupt decline in MS in these cores  $\sim 22$ – $19.5$  ka records

deglaciation in the tropical Andes several thousand years prior to substantial warming at high northern latitudes. However, once glaciers retreated upvalley from end moraines of the LLGM, the moraine-dammed lakes that formed became the principle sediment trap for much of the remainder of the last deglaciation. Thus, cores from Lakes Junin and Titicaca, while providing a critical archive of the timing of initiation of the last deglaciation, cannot be used as an archive of glacier margin fluctuations for much of the past  $\sim 20$  ka.

The Lateglacial interval ( $\sim 14$ – $11$  ka) in the tropical Andes was marked by a minor glacial readvance that has been identified at several sites (Rodbell and Seltzer, 2000, and references therein). The best-dated evidence for this advance comes from bracketing radiocarbon dates at two localities in Peru, which constrain the advance to between  $\sim 13.5 \pm 0.2$  and  $12.9 \pm 0.2$  ka. Many basal radiocarbon dates from lakes and peatlands within several kilometers of cirques provide minimum-limiting ages for deglaciation from Lateglacial ice positions. These dates indicate that ice margins retreated rapidly beginning at least  $\sim 12$  ka, and many valleys with headwall elevations less than 5000 m became ice-free by this time (Seltzer, 1990; Rodbell, 1993a). For example, the Quelccaya Ice Cap (QIC) in southern Peru (Fig. 1) shrank to a size smaller than its modern (pre-AD 1970) size by  $\sim 12$  ka (Mercer and Palacios, 1977).

Records of Neoglaciation differ markedly from region-to-region in the tropical Andes (Rodbell et al., 2008). Basal radiocarbon dates of  $\sim 11,000$  cal yr BP from within 2 km of modern ice margins in many regions of the tropical Andes (e.g., Seltzer, 1990) indicate that glaciers did not expand beyond this limit at any time during the Holocene. Early and middle Holocene moraines have been recognized in only a few regions of the tropical Andes (Clapperton, 1983; Rodbell et al., 2008). Several records suggest that the

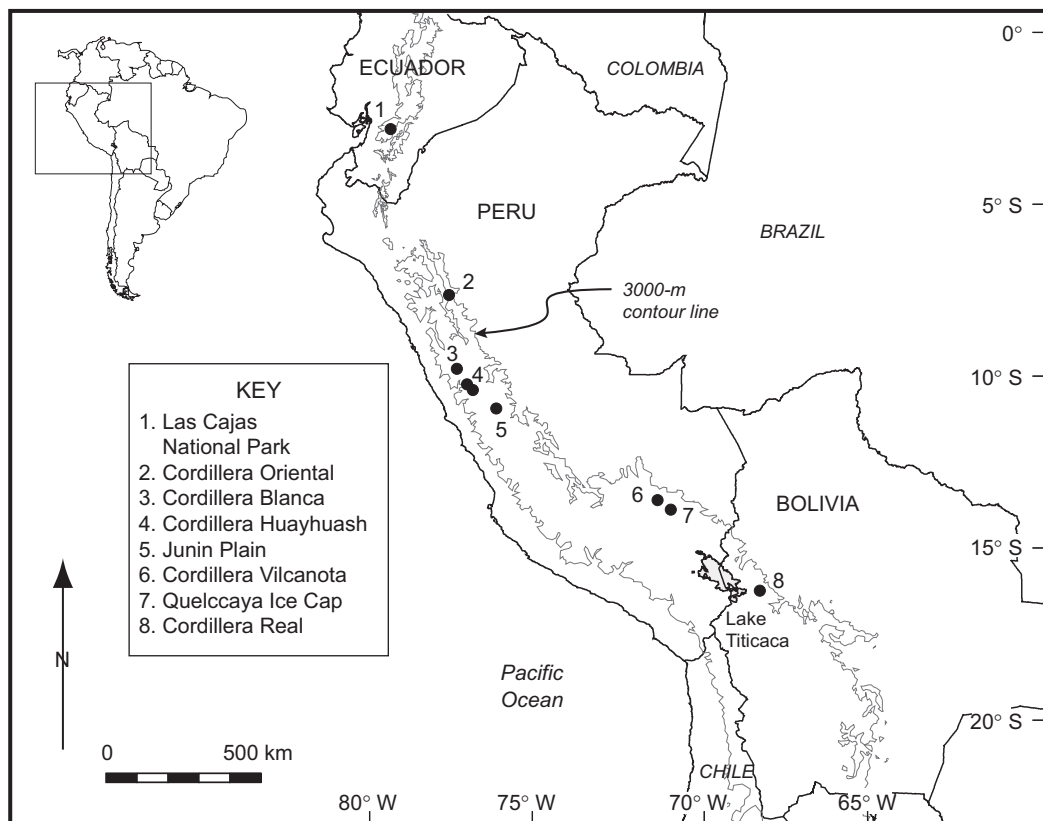


**Fig. 1.** Localities in the tropical Andes where lake cores for this study were acquired. Lakes at each locality are as follows (Table 1): (1) Highest Lake, Chorreras Valley, Pampiada, Chorreras, Llaviucu (Surucocha); (2) Chocho (Negra), Baja; (3) Queshque; (4) Huarmicocha; (5) Junin; (6) Caserococha; (7) Pacococha; (8) Laguna Taypi Chaka Khot.

maximum Neoglacial extent occurred during the late Holocene (~1350 cal yr BP; Wright et al., 1989), several centuries prior to the onset of the Little Ice Age (LIA). In contrast, Röthlisberger (1987) reported radiocarbon dates from wood and buried soils in the Cordillera Blanca of central Peru, and concluded that in addition to ubiquitous late Holocene moraines there are also moraines that date to the early and middle Holocene. Rodbell (1992) reported a four-fold subdivision of Holocene moraines in the Cordillera Blanca based on lichenometry and radiocarbon dating. According to his scenario, early Holocene glaciers advanced as much as 3 km beyond their modern limits, with the maximum extent of Holocene glaciation occurring between 8500 and 6000 cal yr BP. Three younger and less extensive episodes of glaciation occurred ~3500–1800, 1250–400 cal yr BP, and within the last 100 years.

Distinct inter-regional records of late Quaternary glaciation in the tropical Andes may reflect real differences in glacial extent and climate forcing, or may be artifacts of the different proxies used and/or dating methods applied. For example, CRN dating and lichenometry date the time of moraine stabilization whereas basal radiocarbon dates from lakes and peatlands provide minimum-limiting radiocarbon dates for deglaciation from downvalley moraines. A single proxy signal of glaciation from all regions would enable a more rigorous comparison of glaciation from region-to-region in the tropical Andes.

### 1.2. Clastic sediment yield from tropical glaciers

Interest in the erosive capabilities of alpine glaciers was heightened nearly 20 years ago when it was suggested that tectonic uplift and glaciation may impact global climate on time scales of  $\sim 10^{6-7}$  yr by increasing the surface exposure of fresh mineral grains to carbonic acid, thus drawing down atmospheric  $\text{CO}_2$  (Raymo et al., 1988; Raymo and Ruddiman, 1992). This proposed causative linkage between tectonic uplift, glaciation, and global climate change was subsequently turned on its head with the proposal that climate change and glacial erosion may, in fact, drive tectonic uplift (Molnar and England, 1990). Here again, the critical element is glacial erosion, as it was proposed that increased erosion rates in high-elevation areas would drive isostatic rebound of the underlying continental crust, and thus regional mountain-building. Both sides of this chicken-or-egg debate assume that average erosion rates increase during intervals of expanded ice cover, and, implicitly, that a main controlling variable on erosion rates in alpine settings is glaciation.

Estimates of rates of glacial erosion vary widely. In one notable study Hicks et al. (1990) concluded that glacial erosion rates in the Southern Alps of New Zealand are no higher than fluvial erosion rates in the same region. This study was then used to challenge the assumption that glaciation leads to increased erosion rates (Summerfield and Kirkbride, 1992). In addition, Andrews et al. (1994) noted that some East Greenland fjords yield less sediment than river basins of comparable size in Alaska. However, in thoroughly critiquing the Hicks et al. study, Harbor and Warburton (1992, 1993) pointed out that given the difficulty of estimating sediment yields in alpine catchments it is not yet possible to define the relationship between the extent of ice cover and sediment yield. Moreover, these authors noted that the *extent* of glacial cover may not be an accurate surrogate for glacial erosion rates, which are governed principally by ice flow rates, basal thermal regimes, effective normal stress, basal water pressure, and rock type (Hallet, 1979). In their review, Hallet et al. (1996) compiled all available field data on sediment yield by glaciers. Accordingly, sediment yields expressed as effective rates of glacial erosion vary from  $0.001 \text{ mmyr}^{-1}$  for cold-based polar glaciers to  $10\text{--}100 \text{ mmyr}^{-1}$  for high-activity glaciers in the high-relief areas

of southeastern Alaska (Hallet et al., 1996). Throughflow of liquid water in the glacier has a fundamental first-order control on the sediment yield and abrasion of a glacier. Warm-based glaciers in areas of high precipitation are likely to be candidates for greater abrasion (e.g., Østrem, 1975; Hasnain, 1996). This is supported by data from the west slope of the Olympic Mountains, where alpine glaciers have removed two to four times as much rock mass as comparable fluvial valleys in the same geologic and climatic setting (Montgomery, 2002). To date, however, there is little knowledge of glacial erosion rates in the tropics, where some of the highest rates of glacial erosion might be expected to occur.

## 2. Objectives

The objective of this study is to document the flux of clastic sediment to selected alpine lakes in the tropical Andes through the last glacial–deglacial cycle and the Holocene. By comparing this record with independently dated ice margin positions, we attempt to evaluate the role of glaciation in controlling the flux of clastic sediment to tropical Andean lakes. A secondary objective of this study is to identify trends in rates of soil erosion to alpine lakes during the post-glacial interval of the lakes studied. Ultimately, we hope to develop a composite record of clastic sediment flux that can be used as a proxy indicator of glaciation and of climatically-driven changes in soil erosion to alpine lakes in the tropical Andes.

## 3. Methods

We have cored lakes in eight regions in the Peruvian, Ecuadorian, and Bolivian Andes (Fig. 1). These are (from north to south): (1) Las Cajas National Park, southern Ecuador; (2) Cordillera Oriental, northern Peru; (3) Cordillera Blanca, central Peru; (4) Cordillera Huayhuash, central Peru; (5) Junin Plain, central Peru; (6) Cordillera Vilcanota, southern Peru; (7) QIC, southern Peru; and (8) Cordillera Real, northern Bolivia (Table 1). We extracted sediment cores using a square-rod piston corer operated from an inflatable rubber raft (Wright et al., 1984). For this study, we selected the best-dated cores from these regions (Fig. 2).

In the Core Laboratory at Union College (Schenectady, NY, USA), we split, described, and sampled the cores, and measured whole core MS with a 75-mm-diameter core sensor on a Bartington MS2 magnetic susceptibility meter. We chose a variety of sampling intervals depending upon the visual stratigraphy, and in total we analyzed ~2080 samples for bulk density, mass MS, weight percentage total carbon (TC), and weight percentage total inorganic carbon (TIC). For the measurement of TC, we combusted samples at  $1000^\circ\text{C}$  using a UIC 5200 automated furnace, and analyzed the resultant  $\text{CO}_2$  by coulometry using a UIC 5014 coulometer. Similarly, we measured TIC by acidifying samples using a UIC 5240 acidification module and measuring the resultant  $\text{CO}_2$  by coulometry. We calculated weight percentage total organic carbon (TOC) from  $\text{TOC} = \text{TC} - \text{TIC}$ . For ~100 selected samples, we also analyzed for biogenic silica ( $\text{bSiO}_2$ ) following the step-wise extraction technique outlined in DeMaster (1981). Details of analytical procedures are available at: <http://www1.union.edu/~rodbell/CoreLab.html>.

We dated sediment cores using two methods. We used radiocarbon dating by accelerator mass spectrometry (AMS) to date organic matter. In addition, for the sediment cores from southern Ecuador we also applied a regional tephrochronology (Rodbell et al., 2002). We obtained between 5 and 14

**Table 1**  
Summary of lake cores used in compilation of clastic sediment flux calculations

Site (Fig. 1)	Lake identification number (Fig. 2)	Lake	Country	Location (latitude, °)	Location (longitude, °)	Elevation (m a.s.l.)	Elevation of highest cirque headwall above lake	Length of record (cm)	Approximate length of record (cal yr) <sup>a</sup>
1	1a	Highest Lake, Chorreras Valley	Ecuador	2.75	79.14	4020	4500	445	15880
1	1b	Pampiada	Ecuador	2.76	79.26	4100	4500	360	14820
1	1c	Chorreras	Ecuador	2.77	79.16	3700	4500	440	17770
1	1d	Llaviucu (Surucocha)	Ecuador	2.84	79.14	3140	4500	607	12940
1	1e	Pallcacocha	Ecuador	2.77	79.23	4060	4300	963	15000
2	2a	Chochos (Negra)	Peru	7.64	77.47	3285	4200	879	15470
2	2b	Baja	Peru	7.70	77.53	3575	4200	566	18180
3	3	Queshque	Peru	9.82	77.30	4275	5700	1349	18440
4	4	Huarmicocha	Peru	10.43	76.84	4670	5150	700	17350
5	5	Junin	Peru	11.00	76.15	4000	5500	2063	42210
6	6	Caserochocha	Peru	13.66	71.29	3975	6000	832	26270
7	7	Pacocochoa	Peru	13.95	70.88	4925	5650	498	14440
8	8	Taypi Chaka Khota	Bolivia	16.21	68.35	4300	5650	290	13550

<sup>a</sup> Based on combination of polynomial and linear age models (Fig. 2; Table 2).

(average = 8) dates for the 13 cores, and we generated two depth–age models for each core. One age model is a simple linear interpolation between dated intervals, and the other was generated by applying both a polynomial function to the age–depth data (Table 2), and extrapolating the corresponding linear sedimentation rate from the depth of the basal-most radiocarbon age to the bottom of the sediment core. For both age–depth models, we assume that the sediment water interface is contemporaneous with the date that the core was obtained.

We applied a variety of techniques to estimate the flux of the clastic component of sediment in the cores. We calculated the flux of clastic sediment ( $\text{Flux}_{\text{clastic}}$ ) from:

$$\text{Flux}_{\text{clastic}} = \text{SR}(\text{BD} - ((\text{BD} \times \text{TOM}) + (\text{BD} \times \text{TCC})))$$

where SR is the bulk sedimentation rate ( $\text{cm yr}^{-1}$ ), BD the bulk density ( $\text{g cm}^{-3}$ ), TOM the weight fraction organic matter of the bulk sediment, and TCC is the weight fraction authigenic calcite of the bulk sediment. We calculated TOM from  $\text{TOC}(\%)/44$  to reflect the molar ratio between plant cellulose ( $\text{C}_6\text{H}_{10}\text{O}_5$ ) $n$  and TOC (%), and we calculated TCC from  $\text{TIC}(\%)/12$  to reflect the molar ratio between TIC (%) and  $\text{CaCO}_3$ .

We did not measure  $\text{bSiO}_2$  for all samples in all cores. However, we did measure the  $\text{bSiO}_2$  content for samples from Lago Junin and we use the  $\text{bSiO}_2$  data from Abbott et al. (2000) for Laguna Taypi Chaki Khota (LTCK), Bolivia. Data for both records reveals that  $\text{bSiO}_2$  values for pre-Holocene sediments are negligible ( $\leq 1\%$ ) but highly variable for Holocene sediments. The average value for the Holocene section in Lake Junin is 1.9% whereas that for LTCK is  $\sim 39\%$ , and values for random samples from other lakes are  $< 15\%$ . While we do subtract the  $\text{bSiO}_2$  component from the LTCK record in calculating the clastic sediment flux following Abbott et al. (2000), we have not attempted to correct for the  $\text{bSiO}_2$  component of the other lake records. We recognize that this will result in overestimating the clastic flux for the Holocene section of these lakes, but it will have little ( $< 1\%$ ) impact on the pre-Holocene sections of these records. The end result of limited  $\text{bSiO}_2$  data is to underestimate the amplitude of the pre-Holocene to Holocene reduction in clastic sediment flux (discussed below) in all lakes, and to limit the degree to which we can interpret the more subtle apparent shifts in clastic sediment flux to all lakes (except LTCK) during the Holocene. Finally, for the cores from southern Ecuador we removed the tephra layers from the data set

so as to avoid this component in the calculation of clastic sediment flux.

In order to compile numerous records of clastic sediment flux into a single “stacked” record that reflects the regional pattern of clastic sediment input to alpine lakes, we processed each record in the following ways. We calculated a weighted mean flux of clastic sediment to each lake; this was calculated by multiplying the clastic sediment flux determined for each sample in each core by the duration of time represented by that sample, summing these latter values, and dividing this sum by the total time represented in a core. This weighted mean value of clastic sediment flux is thus not unduly affected by short-term intervals of clastic sediment flux that deviate significantly from the mean. Each clastic sediment flux sample for each core was then converted into units of standard deviation ( $z$ -scores) from the weighted mean value for that core. The use of  $z$ -scores is an attempt to remove the site-to-site bias of individual coring sites to record higher or lower long-term sedimentation rates due to basin size, degree of sediment focusing, and/or erosivity of bedrock. Finally, each resultant record was statistically “resampled” at an identical 200-year time step using the Timer program of the ARAND package from Brown University (Providence, RI, USA). This latter resampling step allowed all records to be “stacked” into a composite for the region.

The stacked record of clastic sediment flux to all 13 lakes was then compared with independently dated glacier margin positions to evaluate the relationship between regional ice cover and regional erosion rates. Because the length of the sediment record preserved in a lake as well as the timing and finality of deglaciation of the lake’s drainage basin depends, in part, on the location and elevation of the lake and its associated cirque headwall, we discuss (below) lakes in the following categories: those lakes whose origin predates the LLGM; those with headwall elevations greater than 5000 m; and those with headwall elevations less than 5000 m.

## 4. Results and discussion

### 4.1. Age–depth models

Most cores yield age–depth models that reflect accelerating bulk sedimentation rates through the Lateglacial and Holocene

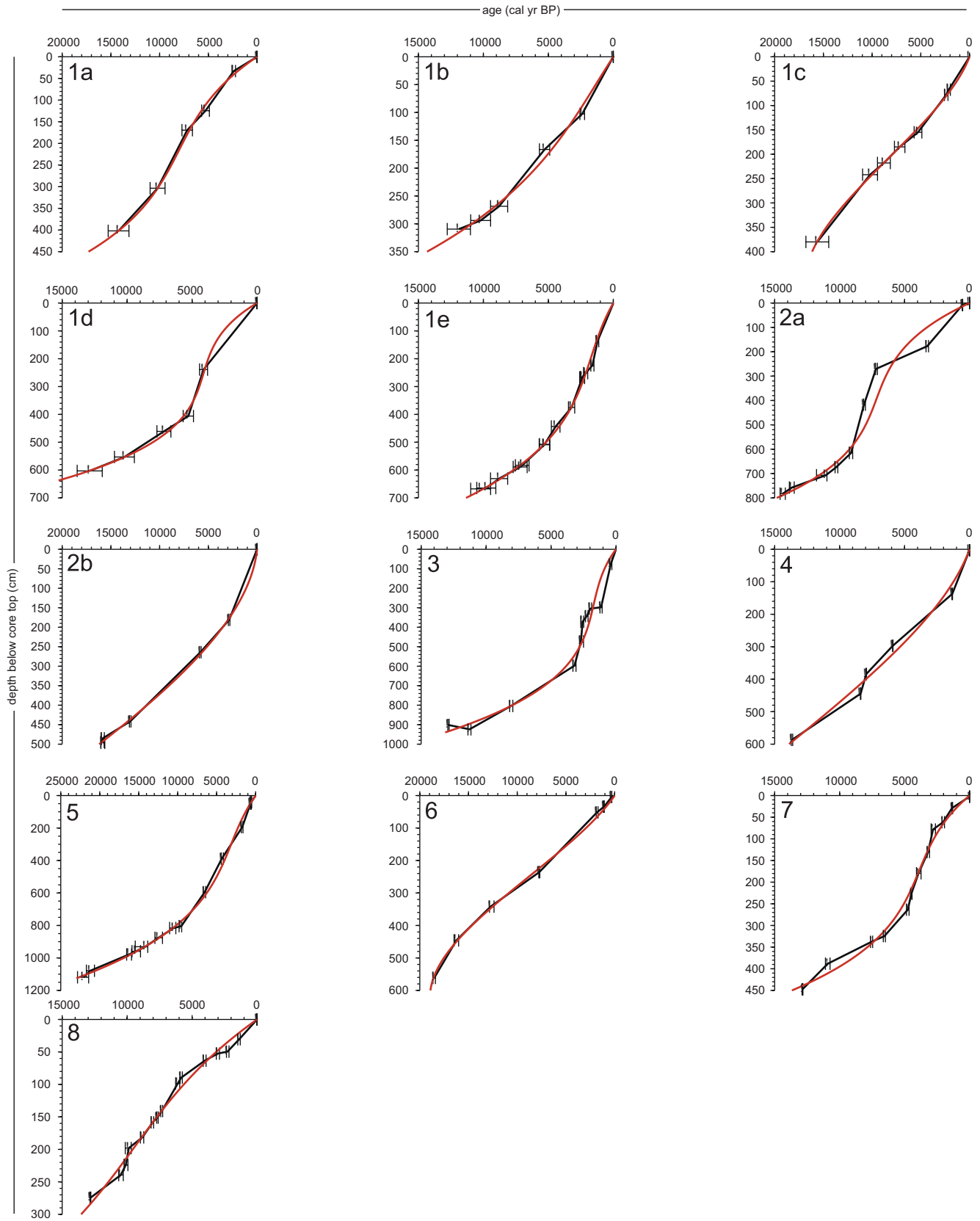


**Fig. 2.** Radiocarbon age–depth relationships for all lake cores used in this study. The numbers in each graph are lake identification numbers in Table 1 and location numbers in Fig. 1. The red curves are based on the polynomial age model in Table 2, and the black curve is based on the linear interpolation between dated intervals.

**Table 2**  
Polynomial age equations used in the calculation of clastic sediment flux

Lake number	Lake	Equation used in polynomial age model ( $X$ is age in cal yr BP; $y$ is depth in cm; Fig. 2)	$r^2$
1a	Highest Lake	$X = 3.1155E-4y^3 - 2.0186E-1y^2 + 6.6178E+1y$	0.80
1b	Pampiada	$X = 1.8688E-4y^3 - 2.8565E-2y^2 + 2.8063E+1y$	0.93
1c	Chorreras	$X = -2.4310E-4y^3 + 1.5018E-1y^2 + 1.9222E+1y$	0.82
1d	Llaviucu (Surucocha)	$X = 1.5298E-4y^3 - 1.1621E-1y^2 + 3.5906E+1y$	0.94
1e	Pallcacocha	$X = 4.7322E-5y^3 - 2.7642E-2y^2 + 1.2352E+1y$	0.99
2a	Chochos (Negra)	$X = 7.2057E-5y^3 - 8.5140E-2y^2 + 4.0544E+1y$	0.82
2b	Baja	$X = -3.7150E-5y^3 + 7.5252E-2y^2 + 4.0632y$	0.97
3	Queshque	$X = 3.2407E-5y^3 - 2.7559E-2y^2 + 1.1277E+1y$	0.97
4	Huarmicocha	$X = -1.8276E-5y^3 + 3.4277E-2y^2 + 9.1626y$	0.87
5	Junin	$X = 2.3122E-5y^3 - 2.0873E-2y^2 + 1.4659E+1y$	0.99
6	Caserococha	$X = -9.9022E-5y^3 + 7.3461E-2y^2 + 2.3083E+1y$	0.78
7	Pacococha	$X = 1.6335E-4y^3 - 6.6953E-2y^2 + 2.6671E+1y$	0.94
8	Taypi Chaka Khota	$X = 2.9188E-4y^3 - 1.7288E-1y^2 + 7.0736E+1y$	0.73

(Fig. 2). This general trend of increasing sedimentation rate over the last 15–20 ka likely reflects a combination of delta progradation, increased sediment focusing, and increased landscape and lacustrine organic productivity that occurred during deglaciation of lake catchments. This increased organic productivity is supported by pollen records from Lagunas Junin (Hansen et al., 1984), Baja (Hansen and Rodbell, 1995), and Chochos (Bush et al., 2005), which show a prominent increase in proximity of Andean Forest vegetation to coring localities during the last deglaciation. Many lakes below 4000 m on the eastern side of the Andes became surrounded by Andean Forest during the early Holocene. The increase in organic productivity in watersheds is also recorded as a pronounced early Holocene increase in the concentration of organic carbon (Rodbell, 1993a; Bush et al., 2005).

In general, it makes little difference whether a linear or polynomial age model is chosen (Fig. 2). The most notable exceptions to this are Lagunas Llaviucu, Chochos, and Queshque (Lakes 1d, 2a, and 3 in Fig. 2), however even small differences in age models result in significant differences in the timing and magnitude of changes in clastic sediment flux. There is no independent way to ascertain which age model is best. Certainly, the use of average sedimentation rates between dated intervals is the simplest approach, but this approach has significant drawbacks. First, it assumes that all radiocarbon dates are accurate and not affected by contamination, or by reservoir or hardwater effects. Secondly, and more importantly, the use of linear sedimentation rates assumes that all changes in sedimentation rate occurred instantly at the time represented by each of the radiocarbon ages. This latter is, of course, unrealistic, and can be clearly seen to produce substantial changes in clastic sediment flux that appear to occur precisely at depths in the core that are dated. We prefer the polynomial age models because they are not unduly affected by any single radiocarbon age, and this approach allocates changes in sedimentation rate gradually between dated intervals. However, polynomial age models also have their shortcomings. First, real information may be lost if an abrupt shift in sedimentation rate actually did occur approximately at the depth of a radiocarbon age but that change in sedimentation rate is smoothed out over a much longer depth interval of the core. An example of this is Laguna Chochos (Lake 2a, Fig. 2). According to the linear age–depth model, a significant increase in sedimentation rate occurred  $\sim 9$  ka, and a decrease occurred  $\sim 7$  ka. The polynomial age model shows more gradual changes in sedimentation that peak later than those in the linear model, and these differences result in significant differences in the clastic sediment flux plots for this lake. The second shortcoming of the polynomial

age model is that because polynomial age models propagate down-core changes in sedimentation rate exponentially back in time, they can yield unrealistically old ages for core bases when unconstrained by data.

For this study, we thus adopted a hybrid approach. For the interval of each core that extends from the sediment–water interface to the depth of the basal-most radiocarbon age, we applied the polynomial age model listed in Table 2. Over this interval, the sedimentation rate used to calculate clastic sediment flux is simply the first-derivative of the polynomial equation in Table 2. Extending downward from the depth of the basal-most radiocarbon age, we extrapolate the average sedimentation rate for the core interval between the basal-most two radiocarbon ages. We recognize that extrapolating beyond the radiocarbon chronology using any age model can yield significant errors. In most cases, we believe that our approach underestimates sedimentation rates for the basal-most parts of most cores because most lakes in this compilation were formed during ice retreat from the moraines that impound them. Thus, the earliest history of these lakes was likely marked by high-sedimentation rates of glacial sediment. The effect of this probable underestimation of sedimentation rates is to underestimate clastic sediment flux during all or part of the basal-most (glacial-most) part of each core.

#### 4.2. Records from lake basins older than 20 ka

In this compilation we include cores from only two alpine lakes that formed more than 20 ka. Lagunas Junin and Caserococha were formed prior to the last glacial cycle in the Andes, and these lakes record sedimentation associated with the LLGM and initial deglaciation from it. Such lakes are rare as most Andean lakes owe their origin to glacial erosion and/or deposition, and, therefore, date to the last deglaciation.

Laguna Junin is located in an intermontane basin between the eastern and western cordillera of the central Peruvian Andes, and formed more than 40 ka when coalescing alluvial fans dammed outflow from the Junin Plain. Radiocarbon dates of more than 43,000  $^{14}\text{Cyr BP}$  have been obtained from depths of  $\sim 28$  m in lacustrine sediment cores (Hansen et al., 1984; Seltzer et al., 2000). During several glacial cycles that predate the LLGM, alpine glaciers from the eastern cordillera formed piedmont lobes that extended to within 1 km of the lake's present eastern margin, but at no time in at least the last several hundred thousand years (Smith et al., 2005c) has the basin been overridden by glaciers.



**Fig. 3.** View looking north of Laguna Caserococha. The lake, which is located at 3975 m on the northwest side of the Cordillera Vilcanota (locality 6, Fig. 1), is about 0.5 km in diameter. During the last glacial cycle, ice flowed from right to left down the valley in the foreground (Río Pinchimuro Mayo), and deposited a nested series of right lateral moraine ridges that are visible in front of Laguna Caserococha (between red arrows). During the LLGM, glacial meltwater flowed from the Río Pinchimuro Mayo into Laguna Caserococha, which, in turn, drained into the Río Tinquimayo drainage, which is visible behind the lake.

Laguna Caserococha (Fig. 3) is located on a till-mantled bedrock interfluvium on the northwest side of the Cordillera Vilcanota in southern Peru, between the Río Pinchimuro Mayo and Río Tinquimayo drainages. Right lateral moraines in the Pinchimuro Mayo drainage indicate that LLGM ice was sufficiently thick that meltwater flowed directly into Laguna Caserococha, which, in turn, drained into Río Tinquimayo (Fig. 3). Step-wise deglaciation from the LLGM ice maxima produced a series of well-preserved lateral moraines below the level of the lake (Fig. 3). Initial deglaciation of the Pinchimuro Mayo valley lowered the ice surface below the level of the lake, and meltwater drainage ceased to enter the lake at that time.

Sediment cores from these two lakes document accelerated clastic sediment flux during the LLGM, and a prominent drop in clastic sedimentation that began ~19 ka (Fig. 4) that records the initial step in the deglaciation of the tropical Andes. By 18 ka glacial flour flux to both basins ceased; that to Laguna Junin because of the formation of moraine-dammed lakes midway down most glacial valleys, which served as the primary glacial sediment traps in the Junin catchment, and that to Laguna Caserococha because the ice surface elevation dropped below the lake surface elevation. The  $bSiO_2$  curve for Junin reveals very low levels during the glacial interval, increasing values during the early Holocene that peak at ~8% (~7 ka), and declining values (<2%) thereafter.

#### 4.3. Records from lake basins <20 ka with headwall elevations >5000 m

Four lakes included in this compilation are from cirque basins that have headwall elevations that exceed 5000 m. These lakes record near complete deglaciation of catchments during the Lateglacial, an early Holocene interval of minimal ice cover, and the onset of Neoglaciation during the mid-late Holocene.

Laguna Pacococha (Table 1; Fig. 5) is located at 4925 m on the northwestern side of the QIC in southern Peru (Fig. 1). As recently as 1997, Laguna Pacococha received meltwater and abundant clastic sediment directly from the QIC, which had a summit elevation of 5650 m at that time. The reduction of clastic sediment flux to Laguna Pacococha from ~14 to 12 ka (Fig. 6) reflects near complete deglaciation of the QIC by ~12 ka, and ice-free conditions with negligible input of clastic sediment (<0.01 g  $cm^{-2} yr^{-1}$ ) continued for much of the interval from ~12 to 5 ka (Fig. 6). At ~5 ka, clastic sediment flux abruptly increased, and reached its maximum for the entire Lateglacial–Holocene interval (~0.1 g  $cm^{-2} yr^{-1}$ ) ~4 ka. From 4 ka to the present, clastic sediment flux to Laguna Pacococha has generally declined.

Radiocarbon-dated ice positions around the QIC confirm that the flux of clastic sediment to Laguna Pacococha is indeed controlled principally by the extent of ice cover. Radiocarbon dates on peat proximal to the modern margin of the QIC indicate

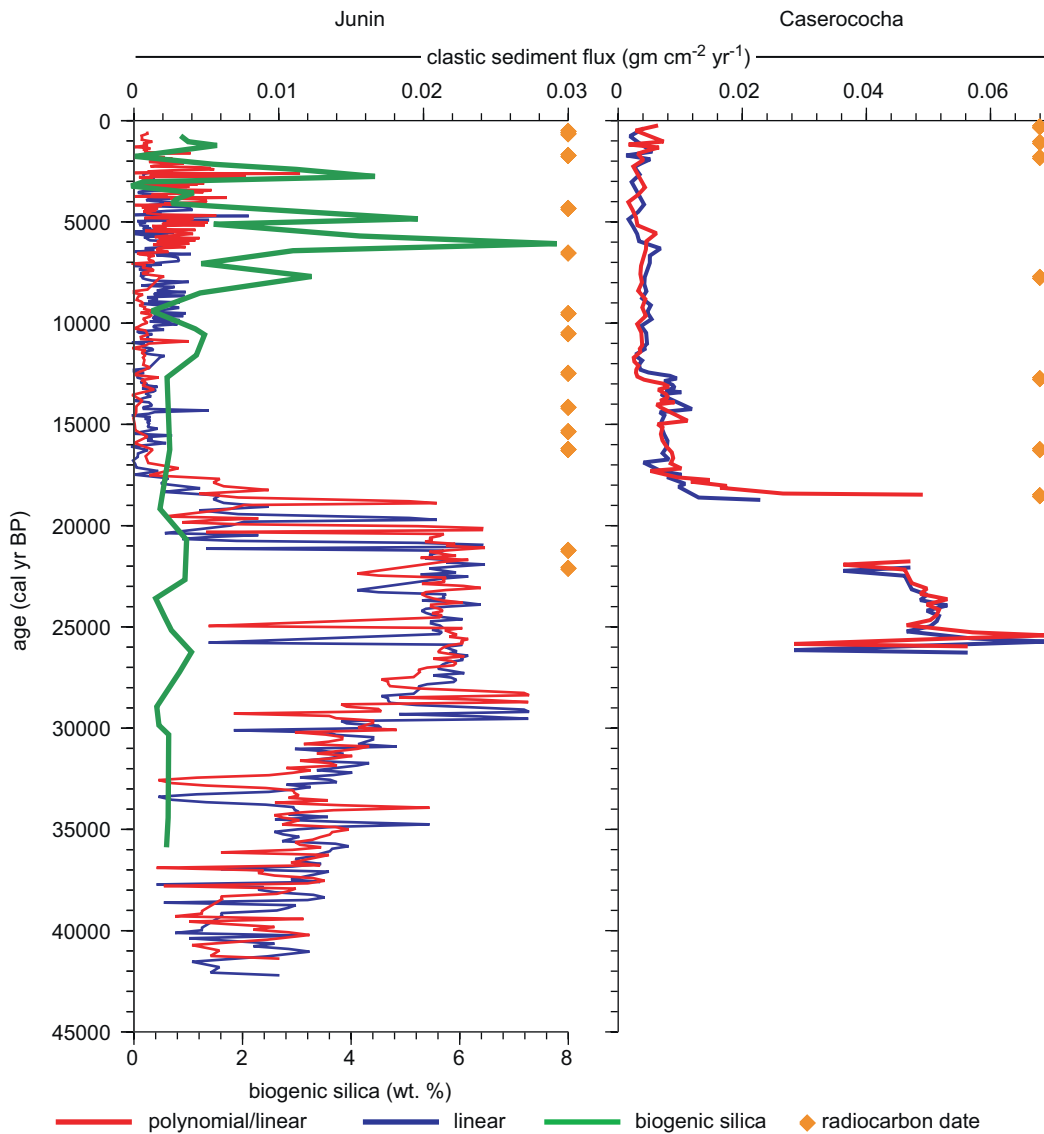


Fig. 4. The record of clastic sediment flux from Lagunas Caserococha and Junin (localities 5 and 6, Fig. 1).

that the QIC was smaller than present from at least  $\sim 11.6$  ka until  $\sim 5.2$  ka. Mercer and Palacios (1977) reported peat exposed beneath late Holocene till within 500 m of the  $\sim$ AD 1975 margin of the QIC; this peat dated to  $9980 \pm 260$   $^{14}\text{C}$  yr BP ( $11,600 \pm 420$  cal yr BP). Thus, this date requires that by 11.6 ka the QIC had retreated from its LLGM position to close to its present size—or smaller—and did not expand more than 500 m beyond its present margin again until the late Holocene. The glacial flour record from Laguna Pacococha indicates that the QIC was, in fact, considerably smaller than the present QIC, and possibly nonexistent, by 12 ka, or earlier. Rodbell and Seltzer (2000) reported radiocarbon evidence for an interval of rapid and nearly complete deglaciation in the tropical Andes that began 12,800 cal yr BP; the glacial flour flux record to Pacococha appears to confirm this. This rapid deglaciation was apparently driven by the onset of more arid conditions in the tropics during the Lateglacial and early Holocene (Abbott et al., 1997; Rodbell and Seltzer, 2000).

A second series of radiocarbon dates (Thompson et al., 2006) date a readvance of the QIC about 5200 cal yr BP. These dates are from cushion plants (*Distichia muscoides*), many in growth position, that have emerged beneath the rapidly-receding margin of the QIC. Apparently, the QIC advanced over the plants without

destroying them  $5135 \pm 45$  cal yr BP, which corresponds closely with the abrupt increase in clastic sediment to Pacococha (Fig. 5). A similar middle Holocene age,  $\sim 4500$  cal yr BP, was reported by Mark et al. (2002) for organic matter buried by glacial sediment in the nearby Cordillera Vilcanota.

The second of the four high-elevation lakes, Laguna Queshque (Table 1), is located at 4000 m on the west side of the Cordillera Blanca in central Peru. The headwall elevation for the Queshque catchment is 5600 m, and numerous moraines are present upvalley from the lake (Rodbell, 1992, 1993b). The record of clastic sediment flux to Laguna Queshque (Fig. 6) reveals minimal clastic sediment flux ( $< 0.05 \text{ g cm}^{-2} \text{ yr}^{-1}$ ) beginning  $\sim 13$  ka and extending through the early Holocene. Clastic sediment flux then increased gradually beginning as early as  $\sim 7$  ka and culminating in maximum rates of clastic sediment input ( $> 0.3 \text{ g cm}^{-2} \text{ yr}^{-1}$ ) by 1450 cal yr BP.

Similar to the Pacococha record, clastic sediment flux to Laguna Queshque appears to reflect the extent of ice cover in the catchment, but significant differences exist between the two records. The peak in clastic sediment flux to Laguna Queshque corresponds closely with a radiocarbon-dated ice margin position in a nearby cirque reported by Rodbell (1992). There, a moraine



**Fig. 5.** View looking to the northeast of Laguna Pacococha with the QIC in the distance (locality 7, Fig. 1). The lake, which is located at 4925 m, is about 500 m wide and receives meltwater directly from the QIC today.

composed almost entirely of peat that had been buckled into an anticline by advancing ice yielded a radiocarbon date of  $1500 \pm 190$  cal yr BP from the stratigraphically uppermost peat (Rodbell, 1992), which is virtually identical to the peak in clastic sediment flux to Laguna Queshque. In the Queshque case, however, the transition from low clastic flux during the early Holocene to much higher flux during the late Holocene occurred more gradually and began somewhat earlier than in the Pacococha record from southern Peru. This more gradual return to glacial flour input may reflect differences in valley hypsometry rather than a fundamentally different climatic transition. The Queshque Valley heads at the crest of the Cordillera Blanca ( $\sim 6000$  m) and relatively less high-elevation terrain is present there than at the QIC, where the ice cap sits on a  $\sim 5500$ -m-high plateau (Mark et al., 2002). Thus, a steadily declining snowline at the end of the early Holocene dry interval would first intersect the high peaks of the Cordillera Blanca, allowing glaciers to grow gradually as snowline descended. In contrast, a gradually descending mid-Holocene snowline would “instantaneously” glaciolate the Quelccaya plateau when snowline descended below the threshold elevation of 5500 m.

The third of the four lakes with high ( $> 5000$  m) headwall elevations is Laguna Huarmicocha, which is located at 4670 m in the Cordillera Huayhuash of central Peru. With a headwall elevation of 5150 m and a maximum summit elevation of 5330 m, this site is similar to the aforementioned Pacococha site

in southern Peru. The flux of clastic sediment to Laguna Huarmicocha is similar to the records from Pacococha and Queshque, but with two significant differences (Fig. 6). Whereas the Huarmicocha clastic sediment record shows a pronounced early Holocene minima and an increase at  $\sim 5$  ka that is also evident in the Pacococha record, the decline in clastic sediment flux to Huarmicocha that began  $\sim 13$  ka was punctuated by a pronounced increase between 12 and 10 ka that is not present in either the Queshque or Pacococha records. Similarly, the minimum from 3 to 2 ka in the Huarmicocha record is not apparent in either of the other high-elevation lake records. These differences may reflect real differences in ice extent or local catchment-specific changes in sediment storage and/or sediment yield from hillslopes.

Laguna Taypi Chaki Khota, at 4300 m elevation, is the oldest of three lakes in the Río Palcoco Valley in the Cordillera Real of Bolivia. With a maximum headwall elevation of 5650 m, this lake is in a setting similar to that of the other lakes in this group. Clastic sediment flux is, however, an order of magnitude lower than for the other high elevation lakes. This is likely due to the fact that LTCK is located downvalley from two other lakes that have served as sediment traps for the bulk of the glacial suspended sediment in the Pacococo Valley throughout the Holocene. Trends in clastic sediment flux through the Lateglacial and Holocene to LTCK are similar to those of the other three lakes in this group. Most notable is the minimum in clastic sediment flux during the

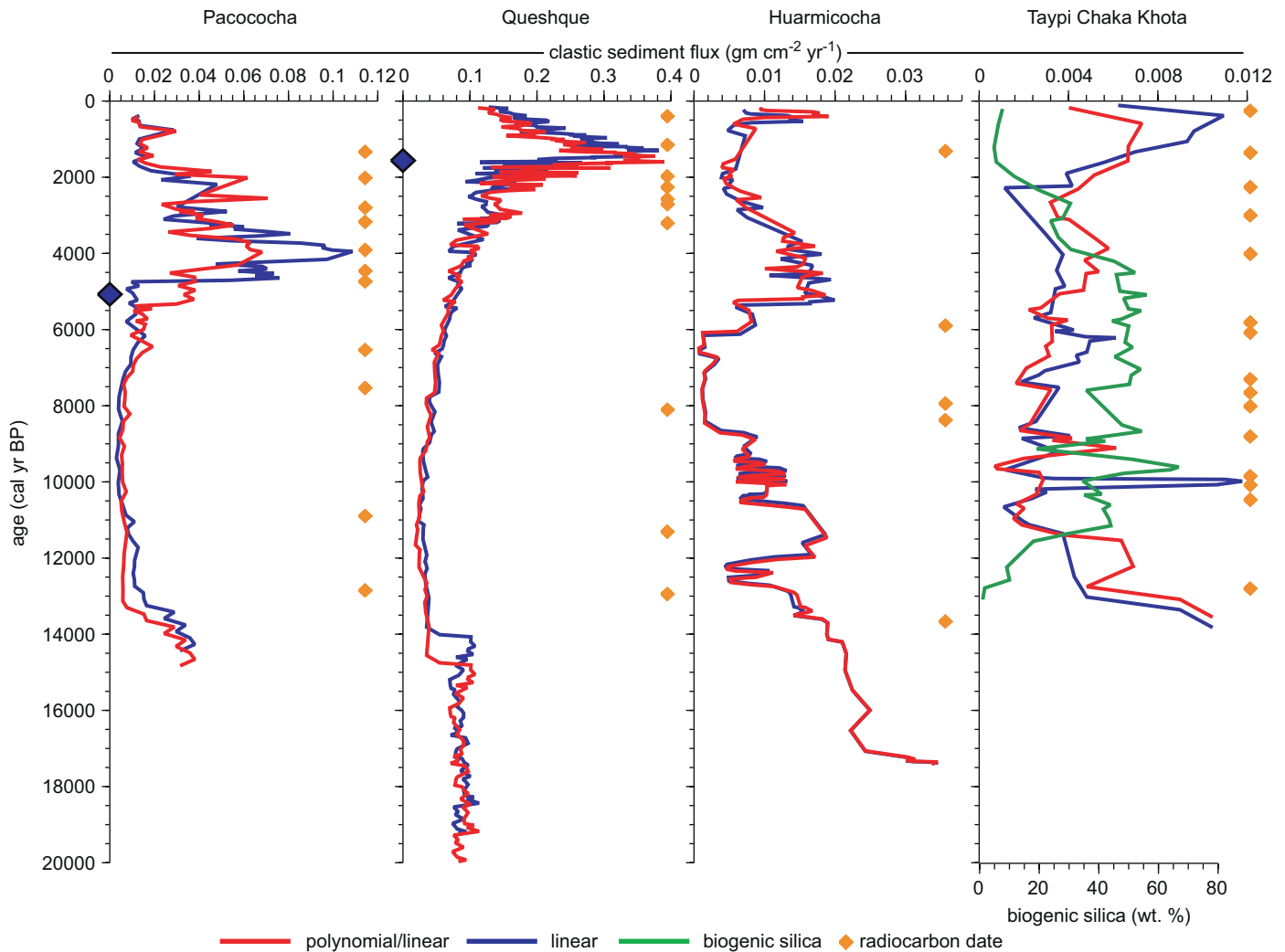


**Fig. 6.** Records of clastic sediment flux from lakes <20 ka with headwall elevations >5000 m. The large blue diamonds in the age scales for Lagunas Pacococha and Queshque indicate the age of organic material overridden by ice advances near these lakes.

early–middle Holocene (8.5–2.5 ka). Though this is apparent in all of the lakes in this group, this interval in LTCK ended later than in the other lakes. Based on analysis of diatoms and the  $\delta^{18}\text{O}$  of plant cellulose from the LTCK core, Abbott et al. (2000) interpreted an interval of aridity between 6 and 2.3 ka, during which time glaciers could not have been present in the LTCK catchment and the lake may have even desiccated on several occasions. After 2.3 ka the diatom and isotopic data indicate wetter conditions and the likely return of glacial ice to the catchment. This latter event is clearly seen in the increased flux of clastic sediment to LTCK that began ~2.5 ka, and culminated in maximum Holocene clastic sediment flux values ~500 cal yr BP.

#### 4.4. Records from lake basins <20 ka with headwall elevations <5000 m

The remaining seven lakes in this compilation are from glaciated catchments with headwall elevations <5000 m. These sites deglaciated early; basal radiocarbon dates from peatlands in the cirque floors of several of these drainages indicate that deglaciation during the Lateglacial was complete and glaciers never reoccupied these catchments at any time in at least the past 12 ka (Seltzer, 1990; Rodbell, 1993a; Rodbell et al., 2002). Thus,

most of the clastic sediment records from these lakes (Fig. 7a and b) must reflect non-glacial processes, with only the interval >12,000 cal yr BP reflecting primary glacial sedimentation.

Among these seven lakes, only Laguna Llavicu in Ecuador (Fig. 7b) does not show elevated clastic sediment flux during the Lateglacial interval. This may be due to the fact that this lake is the lowest elevation (3140 m) lake in the group, and is located downvalley from numerous lakes that would have acted as clastic sediment traps during the Lateglacial interval. With the exception of Laguna Negra in Peru, all lakes show minimum clastic sediment input during the early Holocene, and most lakes show a pronounced increase in clastic sediment input during the late Holocene. Given that glaciers could not have reoccupied these relatively low-elevation catchments, we interpret this latter trend to reflect accelerated landscape erosion during the Lateglacial interval. However, without  $\text{bSiO}_2$  data for all samples from all lakes it is not possible to rigorously interpret the Holocene section of these lakes.

#### 4.5. Composite record of clastic sediment input 40 ka to present

The composite “stacked” record of clastic sediment flux for lakes in the tropical Andes (Fig. 8) was constructed from all 13

lake cores. The earliest part of the record is based on relatively few records (1–3) because most lakes did not form until deglaciation was well underway. The interval from 17 ka to present is based on between six and thirteen records.

The composite record (Fig. 8) reveals a gradual increase in clastic sediment flux from ~40 to 29 ka, an interval of sustained high clastic sediment flux ( $z$ -score values ~2) between 29 and 20 ka, which was followed by a marked decline from 20 to 18 ka during which time  $z$ -score values drop to nearly 0 (the long-term weighted mean). This, in turn, was followed by an abrupt increase in clastic flux between 18 and 17 ka, and sustained moderate clastic sediment flux ( $z$ -score values ~1) between 17 and 14 ka. The Lateglacial interval is marked by steadily declining clastic flux, with  $z$ -score values dropping from ~1 to -0.5 between 14 and 6 ka; these are the lowest clastic flux values in the entire record. Beginning approximately 6 ka, clastic sediment flux increased to reach peak Holocene values about 4 ka, from which they declined steadily to the present.

The  $1\sigma$  envelope about mean  $z$ -score values of clastic sediment flux (Fig. 8) reveals the relative degree of accord among the constituent records. Part of the variation in the  $1\sigma$  envelope is likely due simply to the number of records contributing to particular intervals, with greater error associated with the great-

est number of constituent records. However, it does appear that there may be real significance to the variation in the width of the  $1\sigma$  envelope that is evident in Fig. 8. The Lateglacial and late Holocene are intervals of least agreement among the records, whereas the intervals from ~26 to 18 ka and from ~11 to 5 ka are marked by the greatest agreement among records. The Lateglacial interval may have the greatest variability among records because lakes at different elevations and/or topographic settings became deglaciated at slightly different times with the highest and wettest sites remaining ice-covered the longest. In contrast, the early Holocene features a low level of variance among the 13 constituent records, which all confirm the lowest clastic sediment flux at this time. It is conceivable that this interval was driven by aridity rather than by higher temperatures, given the lack of significant isotopic enrichment in ice cores from Huascaran or Sajama at this time (Thompson et al., 1995, 1998); this agrees with interpretations of the regional hydrology during the early Holocene based on lake records (Abbott et al., 1997, 2000; Seltzer et al., 2000). The termination of this early Holocene arid interval may have been time-transgressive from south to north across the austral tropical Andes. The onset of moister conditions, which caused expansion of Lake Titicaca (Abbott et al., 1997) and the QIC (Thompson et al., 2006) in the south at ~5 ka may not have

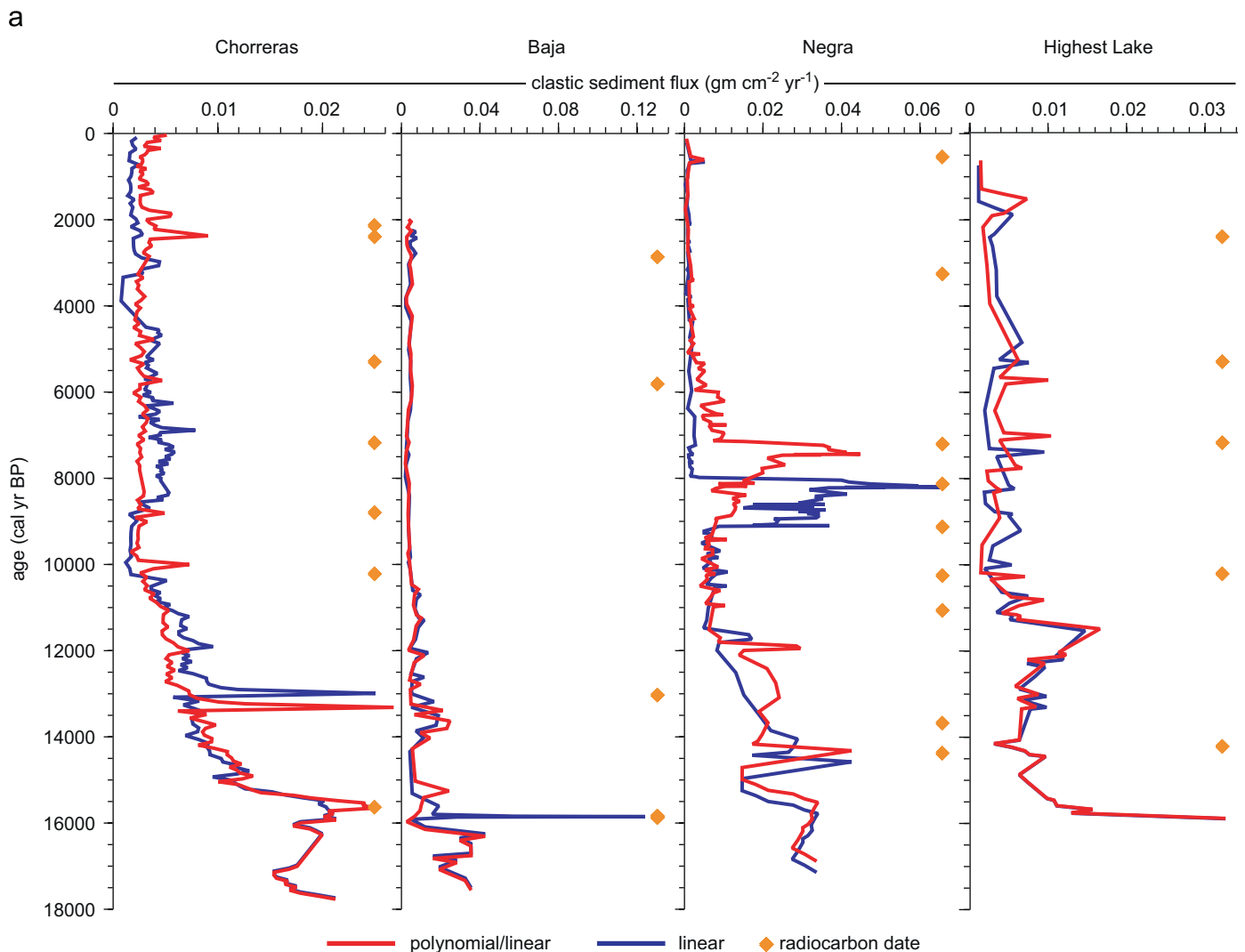


Fig. 7. (a) and (b) Records of clastic sediment flux from lakes <20 ka with headwall elevations <5000 m.

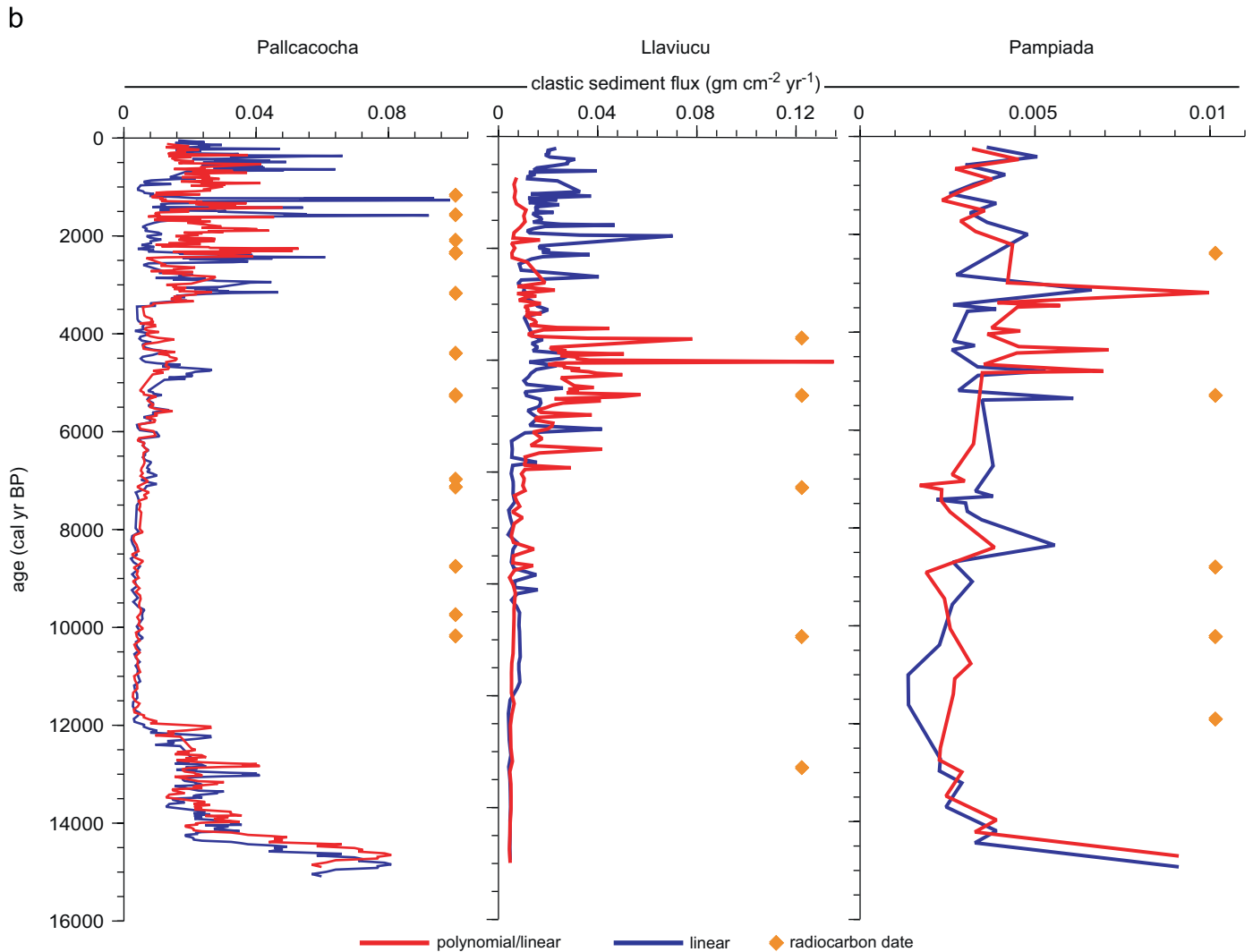


Fig. 7. (Continued)

affected ice cover in northern Peru until ~2 ka, based on records from Lagunas Pacococha and Queshque, respectively. However, as noted above, the difference in the timing of the middle–late Holocene increase in clastic sediment flux at these two lakes may have more to do with catchment hypsometry than with any asynchrony in climatic forcing (Fig. 6).

The end of this early–middle Holocene arid phase appears not only in all lakes in catchments that are high enough to contain active glaciers today (Fig. 6), but also in some lakes from lower elevations that have not had glaciers in their catchments for the entire Holocene. This suggests that the middle–late Holocene paleoclimatic transition not only increased ice cover in the Andes but also resulted in accelerated soil erosion in at least some ice-free catchments. The middle–late Holocene increase in the flux of clastic sediment to alpine lakes in the tropical Andes is similar to the record of El Niño frequency (Rodbell et al., 1999; Moy et al., 2002), and thus may reflect a fundamental change in the nature of ENSO at this time.

There is a striking similarity between the composite clastic sediment flux record and independently dated moraines in the Peruvian and Bolivian Andes (Fig. 9). Not only do the ages of the two aforementioned radiocarbon-dated Holocene moraines (5.1 and 1.6 ka) correspond with peaks in glacial flour flux (Fig. 6), but so too do ~100 CRN ages from erratics on moraine crests (Smith et

al., 2005b,c; Tables S1 and S2; CRN ages recalculated using CRONUS-Earth Online Calculator with time-dependent shielding of Lal, 1991; Stone, 2000; Balco et al., 2008). The oldest group of moraines from the last glacial cycle (Group C in Fig. 9) records ice positions during the LLGM in the tropical Andes. Most of the 37 ages from this moraine group fall between ~30 and 21 ka, with an average of  $25.8 \pm 5.6$  ka ( $\pm 1\sigma$ ; Table S2), which corresponds closely with the broadest peak in clastic sediment flux in the composite record (Fig. 9). The Group C moraines represent a significantly larger glaciation, perhaps as much as 25% larger in aerial extent, than the glaciation that is recorded by the next younger group of moraines, Group B. The 50 CRN ages from the Group B moraines generally fall between ~18 and 14 ka with an average of  $15.2 \pm 2.8$  ka (Smith et al., 2005b,c; Table S2); this corresponds very closely with a pronounced peak in clastic sediment flux (Fig. 9). CRN ages from the youngest moraine group, Group A, which are dominated by ages from the Zongo Valley in Bolivia, fall within the Lateglacial interval, with an average of  $13.4 \pm 2.0$  ka (Smith et al., 2005b,c; Table S2); this too corresponds with a peak in sediment flux (Fig. 9).

The close correspondence among the distribution of CRN ages and variations in clastic sediment flux clearly indicate that a primary control on sediment delivery to alpine lakes in the tropical Andes is glaciation. However, one might expect to see an

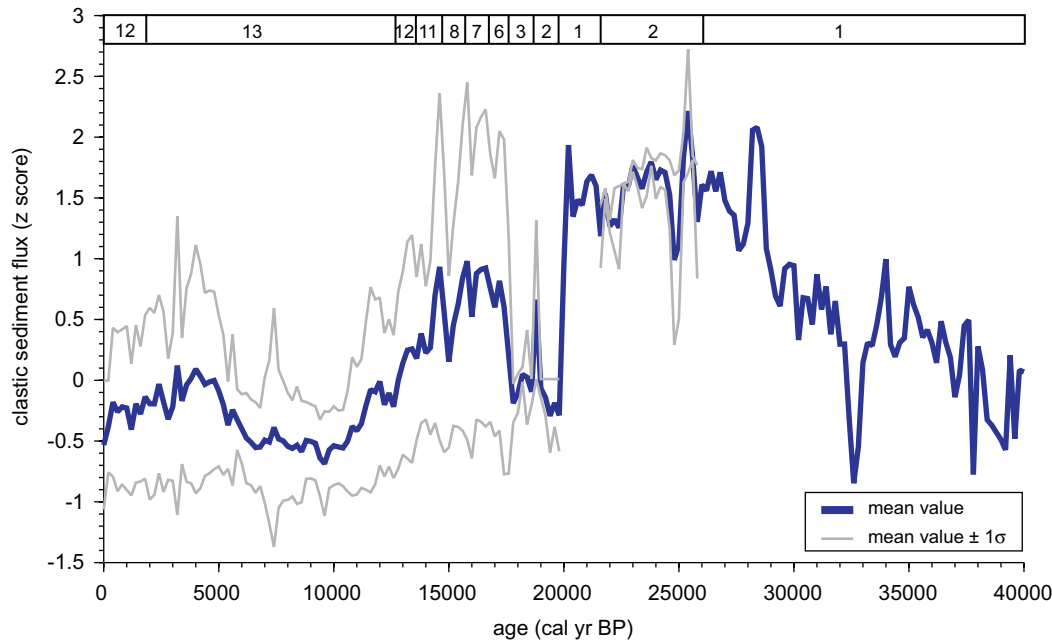


**Fig. 8.** A composite “stacked” record of clastic sediment flux to all lakes in the study. Numbers across the top of the panel refer to the number of records compiled for that interval.

abrupt increase in sediment yield to proglacial lakes during deglaciation and for some time following deglaciation in response to the abundant unvegetated sediment exposed on the landscape. This paraglacial sedimentation (Church and Ryder, 1972) might result in noticeably offset records with the clastic sediment record lagging the moraine record by centuries to millennia. Unfortunately, given the  $\pm 10\%$  uncertainty on the CRN chronology and perhaps a similar uncertainty in the lake records, we cannot demonstrate this offset with the data presented here. More detailed studies of recent deglaciation (last 100–200 years) in the tropical Andes are required in order to document the likely duration of the interval of paraglacial sedimentation in the tropical Andes. Thus, whereas the composite record of glacial clastic sediment flux (Fig. 9) cannot be read simply in terms of the extent of ice cover, it nonetheless reveals that deglaciation from LLGM ice positions was underway by 20 ka, or somewhat earlier. This, in turn, confirms assertions made by Seltzer et al. (2002) and Smith et al. (2005b, c) that the onset of deglaciation in the tropical Andes preceded that in the Northern Hemisphere by several thousand years.

## 5. Conclusions

Clastic sediment flux to alpine lakes in the tropical Andes can be used as a proxy indicator of the extent of regional ice cover. The close correlation between peaks in clastic sediment flux and radiometric ages of moraines indicates that basin-specific factors that might complicate such a relationship, such as changes in sediment storage or paraglacial lag times, are not significant on the  $10^3$ -year time scale of this study.

Lakes that predate the LLGM record an increase in clastic sediment input that began more than  $\sim 40$  ka and culminated in peak sediment flux  $\sim 29$ – $20$  ka; this correlates closely with the age of stabilization of LLGM moraines in central Peru and northern Bolivia. The subsequent decline in clastic sediment flux began  $\sim 20$  ka, and this appears to mark the onset of ice retreat in the region, which preceded warming in the high latitudes of the

Northern Hemisphere by at least one millennia. This early deglaciation in the tropical Andes appears to have occurred under moist conditions based on the relatively high water levels of Altiplano lakes at the time (Seltzer et al., 2002; Placzek et al., 2006), and thus it was most likely driven by increased temperatures. The notion that warming in the tropics may have led warming in the high latitudes of the Northern Hemisphere bolsters questions about the role of the tropics as a source of direct forcing as well as feedbacks in the global climate system (e.g., Cane, 1998).

Clastic sediment flux to alpine lakes during the Lateglacial and Holocene also corresponds with available radiometric ages for moraines in the region. Accordingly, the Lateglacial period was punctuated by an ice advance centered on  $\sim 16$  ka, which was followed by ice retreat to near modern limits by 12 ka. This final deglaciation may have been driven principally by the onset of arid conditions in the tropical Andes. The lowest levels of clastic sediment flux to alpine lakes in the past  $\sim 40$  ka occurred during the early Holocene, and glaciers did not significantly readvance until  $\sim 5$  ka or later. This readvance and the concomitant increase in clastic sediment flux appear to have been associated with an increase in effective moisture. Variation in non-glacial clastic sediment flux to alpine lakes during the Holocene also appears to reflect the significant mid-Holocene transition that is evident in the glacial lake records. The onset of wetter conditions coupled with an increase in the vigor of the ENSO cycle may have promoted increased soil erosion and sediment yield in the region. However, the role of anthropogenic activities during this time, which is apparent in many pollen records from the region (e.g., Hansen and Rodbell, 1995), may complicate the relationship between climate and sediment yield during the middle–late Holocene.

## Acknowledgements

Research was supported by grants from the US National Science Foundation (EAR-9418886 and ATM-9809229 to D.T.R.,

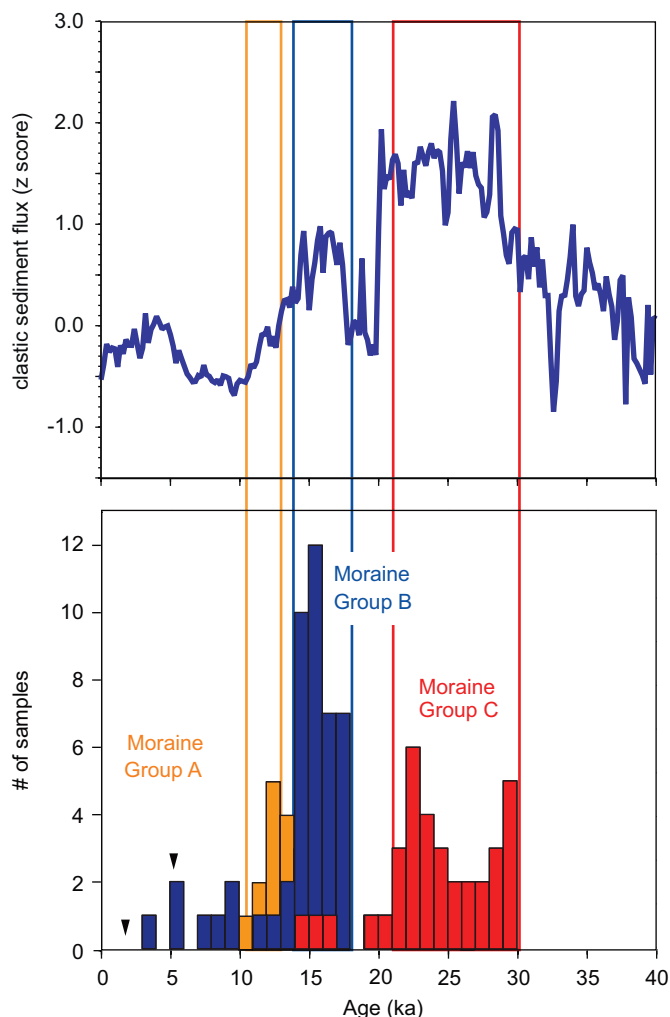


**Fig. 9.** Comparison of stacked record of clastic sediment flux (from Fig. 8) with the distribution of CRN ages from erratics on three different moraine groups on the Junin Plain, Peru (locality 5, Fig. 1) and in the Milluni and Zongo Valleys, Bolivia (locality 8, Fig. 1; from Smith et al., 2005a). Moraine Group C demarcates the ice limit of the LLGM in the region. CRN ages were recalculated using the CRONUS-Earth online calculator (Balco et al., 2008) and the time-dependent scaling method of Lal (1991) and Stone (2000).

and EAR-9422424 and ATM-9813969 to G.O.S.), and from the National Geographic Society. This manuscript benefited from a very thorough review by Pratiya Polissar, and from comments from an anonymous reviewer. We are grateful to the late Alcides Ames of Huaraz, Peru, and his family for many years of logistical support.

## Appendix A. Supplementary Materials

Supplementary data associated with this article can be found in the online version at doi:10.1016/j.quascirev.2008.06.004.

## References

Abbott, M.B., Seltzer, G.O., Kelts, K.R., Southon, J., 1997. Holocene paleohydrology of the tropical Andes from lake records. *Quaternary Research* 47, 70–80.

- Abbott, M.B., Wolfe, B.B., Aravena, R., Wolfe, A.P., Seltzer, G.O., 2000. Holocene hydrological reconstructions from stable isotopes and paleolimnology, Cordillera Real, Bolivia. *Quaternary Science Review* 19, 1801–1820.
- Andrews, J.T., Milliman, J.D., Jennings, A.E., Rynes, N., Dwyer, J., 1994. Sediment thicknesses and Holocene glacial marine sedimentation rates in three East Greenland Fjords (ca 68°N). *Journal of Geology* 102, 669–683.
- Balco, G., Stone, J.O.H., Lifton, N.A., Dunai, T.J., 2008. A complete and easily accessible means of calculating surface exposure ages or erosion rates from  $^{10}\text{Be}$  and  $^{26}\text{Al}$  measurements. *Quaternary Geochronology* 3, 174–195.
- Bush, M.B., Hansen, B.C.S., Rodbell, D.T., Seltzer, G.O., Young, K.R., Léon, B., Abbott, M.B., Silman, M.R., Gosling, W.D., 2005. A 17,000-year history of Andean climate and vegetation change from Laguna de Chochos, Peru. *Journal of Quaternary Science* 20, 703–714.
- Cane, M.A., 1998. A role for the tropical Pacific. *Science* 282, 59–61.
- Church, M., Ryder, J.M., 1972. Paraglacial sedimentation: a consideration of fluvial processes conditioned by glaciation. *Geological Society of America Bulletin* 83, 3059–3071.
- Clapperton, C.M., 1983. The glaciation of the Andes. *Quaternary Science Reviews* 2, 83–155.
- DeMaster, D.J., 1981. The supply and accumulation of silica in the marine environment. *Geochimica et Cosmochimica Acta* 45, 1715–1732.
- Hallet, B., 1979. A theoretical model of glacial abrasion. *Journal of Glaciology* 23, 39–50.
- Hallet, B., Hunter, L., Bogen, J., 1996. Rates of erosion and sediment evacuation by glaciers: a review of field data and their implications. *Global and Planetary Change* 12, 213–235.
- Hansen, B.C.S., Rodbell, D.T., 1995. A late-glacial/Holocene pollen record from the eastern Andes of northern Peru. *Quaternary Research* 44, 216–227.
- Hansen, B.C.S., Wright Jr., H.E., Bradbury, J.P., 1984. Pollen studies in the Junin area, central Peruvian Andes. *Geological Society of America Bulletin* 95, 1454–1465.
- Harbor, J.M., Warburton, J., 1992. Glaciation and denudation rates. *Nature* 356, 751.
- Harbor, J., Warburton, J., 1993. Relative rates of glacial and nonglacial erosion in alpine environments. *Arctic and Alpine Research* 25, 1–7.
- Hasnain, S., 1996. Factors controlling suspended sediment transport in Himalayan glacier meltwaters. *Journal of Hydrology* 181, 49–62.
- Hicks, D.M., McSaveney, M.J., Chinn, T.J.H., 1990. Sedimentation in proglacial Ivory Lake, Southern Alps, New Zealand. *Arctic and Alpine Research* 22, 26–42.
- Lal, D., 1991. Cosmic ray labeling of erosion surfaces; in situ nuclide production rates and erosion models. *Earth and Planetary Science Letters* 104, 424–439.
- Mark, B.G., Seltzer, G.O., Rodbell, D.T., Goodman, A.Y., 2002. Late glacial and Holocene deglaciation in the Cordillera Vilcanota-Quelccaya Ice Cap region, SE Peru. *Quaternary Research* 57, 287–298.
- Martinson, D.G., Pisias, N.G., Hays, J.D., Imbrie, J., Moore, T.C., Shackleton, N.J., 1987. Age, dating and the orbital theory of the Ice Ages: development of a high resolution 0 to 300,000-year chronostratigraphy. *Quaternary Research* 27, 1–29.
- Mercer, J.H., Palacios, M.O., 1977. Radiocarbon dating of the last glaciation in Peru. *Geology* 5, 600–604.
- Mix, A.C., Bard, E., Schneider, R., 2001. Environmental processes of the ice age: land, oceans, glaciers (EPILOG). *Quaternary Science Reviews* 20, 627–658.
- Molnar, P., England, P., 1990. Late Cenozoic uplift of mountain ranges and global climate change: chicken or egg? *Nature* 346, 29–34.
- Montgomery, D.R., 2002. Valley formation by fluvial and glacial erosion. *Geology* 30, 1047–1050.
- Moy, C.M., Seltzer, G.O., Rodbell, D.T., Anderson, D., 2002. Subdecadal-millennial scale variability in the El Niño Southern Oscillation as recorded in lake sediments from southern Ecuador. *Nature* 420, 162–165.
- Østrem, G., 1975. Sediment transport in glacial meltwater streams. In: Jopling, A.V., McDonald, B.C. (Eds.), *Glaciofluvial and Glaciolacustrine Sedimentation*, Special Publication 23. Society of Economic Palaeontologists and Mineralogists, Tulsa, OK, pp. 101–122.
- Placzek, C., Quade, J., Patchett, P.J., 2006. Geochronology and stratigraphy of late Pleistocene lake cycles on the southern Bolivian Altiplano: implications for causes of tropical climate change. *Geological Society of America Bulletin* 118, 515–532.
- Raymo, M.E., Ruddiman, W.F., 1992. Tectonic forcing of late Cenozoic climate. *Nature* 359, 117–122.
- Raymo, M.E., Ruddiman, W.F., Froelich, P.N., 1988. Influence of late Cenozoic mountain building on ocean geochemical cycles. *Geology* 16, 649–653.
- Rodbell, D.T., 1992. Lichenometric and radiocarbon dating of Holocene glaciation, Cordillera Blanca Perú. *The Holocene* 2, 19–29.
- Rodbell, D.T., 1993a. The timing of the last deglaciation in Cordillera Oriental, northern Peru based on glacial geology and lake sedimentology. *Geological Society of America Bulletin* 105, 923–934.
- Rodbell, D.T., 1993b. Subdivision of late Pleistocene moraines in the Cordillera Blanca, Perú based on rock weathering features, soils and radiocarbon dates. *Quaternary Research* 39, 133–143.
- Rodbell, D.T., Seltzer, G.O., 2000. Rapid ice margin fluctuations during the Younger Dryas in the tropical Andes. *Quaternary Research* 54, 328–338.
- Rodbell, D.T., Seltzer, G.O., Anderson, D.M., Abbott, M.B., Enfield, D.B., Newman, J.H., 1999. A ~15,000-year record of El-Niño driven alluviation in southwestern Ecuador. *Science* 283, 516–520.
- Rodbell, D.T., Bagnato, S., Nebolini, J., Seltzer, G.O., Abbott, M.B., 2002. A Late Glacial–Holocene tephrochronology for glacial lakes in southern Ecuador. *Quaternary Research* 57, 343–354.

- Rodbell, D.T., Smith, J.A., Mark, B.G., 2008. Glaciation in the Andes during the Late Glacial and Holocene. *Quaternary Science Reviews*, under review.
- Röthlisberger, F., 1987. 10,000 Jahre Gletschergeschichte der Erde: Aarau, Verlag Sauerländer, 348p.
- Seltzer, G.O., 1990. Recent glacial history and paleoclimate of the Peruvian-Bolivian Andes. *Quaternary Science Reviews* 9, 137–152.
- Seltzer, G., Rodbell, D., Burns, S., 2000. Isotopic evidence for late Quaternary climatic change in tropical South America. *Geology* 28, 35–38.
- Seltzer, G.O., Rodbell, D.T., Baker, P.A., Fritz, S.C., Tapia, P.M., Rowe, H.D., Dunbar, R.B., 2002. Early warming of tropical South America at the last glacial–interglacial transition. *Science* 296, 1685–1686.
- Smith, J.A., Seltzer, G.O., Rodbell, D.T., Klein, A.G., 2005a. Regional synthesis of last glacial maximum snowlines in the tropical Andes, South America. *Quaternary International* 138/139, 145–167.
- Smith, J.A., Finkel, R.C., Farber, D.L., Rodbell, D.T., Seltzer, G.O., 2005b. Early local last glacial maximum in the tropical Andes. *Science* 308, 678–681.
- Smith, J.A., Finkel, R.C., Farber, D.L., Rodbell, D.T., Seltzer, G.O., 2005c. Moraine preservation and boulder erosion in the tropical Andes: interpreting old surface exposure ages in glaciated valleys. *Journal of Quaternary Science* 20, 735–758.
- Stocker, T.F., 2002. North–south connections. *Science* 297, 1814–1815.
- Stone, J.O., 2000. Air pressure and cosmogenic isotope production. *Journal of Geophysical Research, B, Solid Earth and Planets* 105, 23,753–23,759.
- Summerfield, M.A., Kirkbride, M.P., 1992. Climate and landscape response. *Nature* 355, 306.
- Thompson, L.G., Mosley-Thompson, E., Davis, M.E., Lin, P.-N., Henderson, K.A., Cole-Dai, J., Bolzan, J.F., Liu, K.-B., 1995. Late glacial stage and Holocene tropical ice core records from Huascarán, Perú. *Science* 269, 46–50.
- Thompson, L.G., Davis, M.E., Mosley-Thompson, E., Sowers, T.A., Henderson, K.A., Zagorodny, V.S., Lin, P.-N., Mikhalenko, V.N., Campen, R.K., Bolzan, J.F., Cole-Dai, J., Francou, B., 1998. A 25,000-year tropical climate history from Bolivian ice cores. *Science* 282, 1858–1864.
- Thompson, L.G., Mosley-Thompson, E., Brecher, H., Davis, M., Leon, B., Les, D., Lin, P.-N., Mashiotta, T., Mountain, K., 2006. Abrupt tropical climate change: past and present. *Proceedings of the National Academy of Sciences* 103, 10536–10543.
- Wright Jr., H.E., Mann, D.H., Glaser, P.H., 1984. Piston corers for peat and lake sediments. *Ecology* 65, 657–659.
- Wright Jr., H.E., Seltzer, G.O., Hansen, B.C.S., 1989. Glacial and climatic history of the central Peruvian Andes. *National Geographic Research* 5, 439–446.